SAND2017-9601C

In-situ measurement of Gamma Radiation Induced Conductivity of $BaTiO_3$ and Ce-doped $BaTiO_3$

Jonathan A. Bock* and Harlan Brown-Shaklee
Sandia National Laboratories, Albuquerque, NM 87123
e-mail: Jabock@Sandia.gov

Leakage of $BaTiO_3$ due to gamma irradiation is studied in-situ via resistance measurements under multiple radiation dose rates, and the effect of Ce doping is investigated. $BaTiO_3$ exhibits photoconduction under gamma irradiation, and a gamma dose-rate dependence of the radiation induced conductivity has a power exponent of ~0.5-0.6. We have shown that settling time errors can significantly affect the radiation induced conductivity-gamma measurments. The addition of deep traps via substituting Ce onto the Ti site in $BaTiO_3$ reduced the radiation induced conductivity by ~30-40%.
Key words: Radiation Hardness, Capacitors, Radiation-Induced Leakage Currents

1. INTRODUCTION

Ferroelectric capacitors under ionizing radiation suffer from many deleterious effects. For example, gamma radiation from ^{60}Co will increase the defect density in ferroelectrics which will result in pinning domain walls, thereby decreasing the dielectric constant and remnant polarization. [1] Additionally, capacitors will discharge due to free carrier creation via activation of electrons across the band gap leading to significant leakage currents. Understanding and ultimately minimizing these effects are important for capacitors used in radioactive environments including extraterrestrial satellites, nuclear reactors, or robotics used for radioactive waste cleanup. While may studies have focused on ex-situ measurements of ferroelectric capacitors post gamma radiation exposure [2-4] comparatively little study has been performed on the in-situ effects of radiation on capacitor materials, such as radiation-induced leakage currents. [5]

One requirement for radiation hard capacitors is the minimization of capacitor self-discharge under dose accumulation. This self-discharge is controlled by the RC time constant of the capacitor. As both R, resistance, and C, capacitance, have inversely proportional geometric factors, the RC time constant is geometrically independent and is given by:

$$RC = \frac{\varepsilon_r \varepsilon_o}{\sigma_{RIC}} \quad \text{(Eq. 1)}$$

where ε_r is the relative permittivity, ε_o is the permittivity of free space, and σ_{RIC} is the conductivity of the sample under radiation (radiation-induced conductivity). The time to discharge can therefore be minimized by 1) increasing the dielectric constant of the dielectric or 2) decreasing the radiation induced conductivity. The latter of these is the focus of the current research.

The origin of radiation induced conductivity is the interaction of the material with the high-energy radiative particles, with a focus here on gamma irradiation, have energies (often MeV) much greater than the band gap of common ferroelectrics (~3eV), resulting in free electron creation. Given the presence of mobile charge carriers, this radiation induced conductivity can be split into the nominal components:

$$\sigma = ne\mu \quad \text{(Eq. 2)}$$

where n is the carrier concentration, e is the charge of the charge carrier, and μ is the charge carrier mobility. While σ_{RIC} should follow this common law, complications arise compared to nominal photoconductors.

In a photoconductor the carrier concentration can be a function of trap density, defect capture cross section, rate of reemission from shallow carriers, and the nature of lattice relaxation around deep trap states [6]. However, due to damage cascade process upon gamma-ray absorption, a large number of electron-hole pairs are made in close proximity and a large amount of geminate recombination occurs [7] which likely makes additional factors such as the applied electric field, local ferroelectric field magnitude, and dielectric constant important parameters. The complicated nature of the phenomenon along with the overall lack of widespread access to equipment suitable for in-situ measurement of conductivity under gamma irradiation environments makes for a dearth of fundamental knowledge about the subject with a scattered literature. [8] We therefore have started to undertake a systematic study of radiation induced conductivity in $BaTiO_3$ to better understand the phenomenon with the eventual goal of increasing the radiation hardness of ceramic capacitors.

Here we present initial work toward this goal: the first systematic measurements of radiation induced conductivity of $BaTiO_3$ and Cerium-doped $BaTiO_3$. Ce was chosen as a dopant due to a clear understanding of its energy level [9] due to its use in photorefractive crystals, as well as its nature as a deep trap (1.5eV) which should minimize trapped carrier re-emission.

2. EXPERIMENTAL

Samples of $BaTiO_3$ and $Ba(Ce_{0.05},Ti_{0.95})O_3$ were fabricated by solid state reaction of $BaCO_3$ (99.8%, Aldrich), TiO_2(99%, Strem Chemicals), and CeO_2(99.9%, Aldrich). Correct ratios of the precursors were mixed via

ball milling with ~2mm diameter ZrO_2 milling media in ethanol in a high density polyethylene bottle. Mixed powders were dried via rotoevaporation and calcined at 900°C for 6hrs. Calcined powders were ball milled in DI water for 24hrs by the same method as mixing. At the end of milling PVA-PEG was added to the ceramic-water mixture which was subsequently frozen using a shell bath after which the ice was sublimed using a vacuum manifold. The resulting powder was pressed via uniaxial pressing at ~13MPa, followed by cold isostatic pressing at ~120MPa. The binder was removed via heating to 500°C at 3°C/min and holding for 5 hours. The resulting pellets were sintered at 1350°C resulting in pellets with >95% relative density. The pellets were electroded with Cr/Au electrodes and the dielectric constant and loss were measured from room temperature to 140°C, showing nominal dielectric response [10] with and $\tan\delta<0.02$ at 1kHz.

The Gamma Irradiation Facility (GIF) at Sandia National Labs was utilized for radiation exposure (Fig. 1). GIF contains of an array of ^{60}Co sources which can be raised into a 5.5x9.1m room via a lift. The gamma dose rate was controlled by distance from the array using an simple motor controlled movable platform. Gamma ray dose rates were measured using an ion chamber mounted next to the sample equidistant from the ^{60}Co array. Current induced via the radiation environment in cabling and fixtures was measured and found to be nominally ~+-5pA, although transient spikes of 20pA were identified during initial doses.

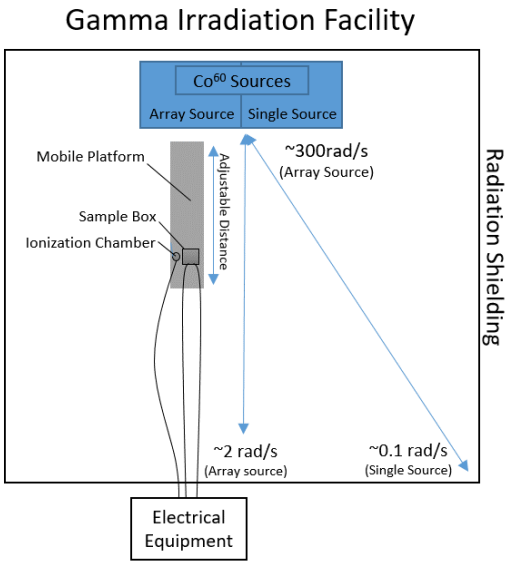

Fig. 1. Layout of experiment within Gamma Irradiation Facility. Sample is positioned using a movable platform at different distances from ^{60}Co source to obtain different gamma dose rates.

The electrode pattern on samples was designed for in-situ radiation measurements. One side of the sample was covered with a blanket electrode. The other side was patterned with an inner circle electrode surrounded by a ring along the outer edge of the sample. The outer ring acted as a guard electrode to prevent conductivity from surface conduction along the edge of the sample during measurements under radiation. (Cracking of airborne hydrocarbons can deposit on surfaces and cause large surface conductivities under radiative environments [11]). Measurements of conductivity under radiation were performed using a Keithly 2401 source-measure unit to apply 5-20 volts to the blanket electrode while a HP4140B picoammeter was used to measure the current through the inner electrode. The guard ring was connected to the inner shield of the triax cable which shorted to ground outside of the radiation chamber. This effectively prevented surface conduction contributions from entering the picoammeter. The inner shield of a triax cable connected to the Keithly 2401 was driven to prevent voltage drops on the center pin. Samples were contained in metal boxes to prevent RF noise and minimize air ionization contributions. Note that all reported dose rates are applied dose rates and not absorbed dose rates.

3. RESULTS AND DISCUSSION

Initial measurements were taken during the onset of gamma irradiation. Fig. 2 shows the current passing through $BaTiO_3$ under a 20V application as a function of time while the gamma ray source is lifted into the chamber (note the log-log axes).

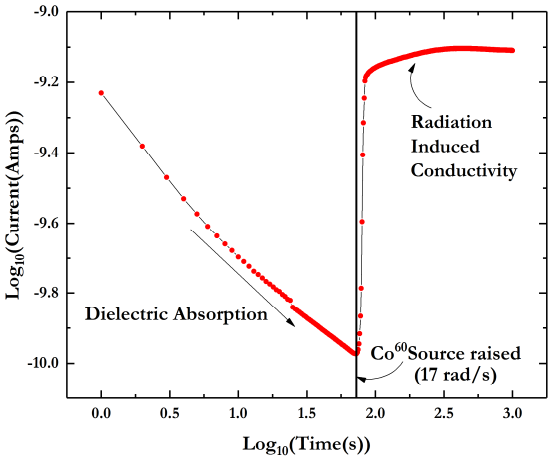

Fig. 2. Current passing through $BaTiO_3$ as a function of time before and during gamma irradiation.

Before the application of gamma irradiation, the current passing through the sample decreases roughly linearly on a log-log scale as is expected via the Curie Von Schweidler law, and is therefore attributed to dielectric absorption as well as sample and cable charging. Upon application of the gamma radiation field, the current through the sample increases significantly.

It should be noted that at these dose rates the initial current from charging and dielectric absorption and the radiation induced conductivity are similar in magnitude. Therefore, it is important to take the dielectric absorption into account during measurement of σ_{RIC}. A series of current vs time plots for multiple dose rates are plotted for a $BaTiO_3$ sample in Fig. 3. Note that the curves are offset so that the initial currents are equal.

At short times the charging and dielectric absorption currents are high, and these outweigh the current from σ_{RIC}. As time increases both the charging and dielectric absorption current decrease. For higher radiation doses

(ex. 216rad/s in Fig. 3) the conductivity for RIC takes over within a few hundred seconds and σ_{RIC} can be properly measured. For lower dose rates (ex. 44rad/s and 17rad/s in Fig. 3), even after 300s, the current has not settled to a continuous value and therefore the calculated σ_{RIC} is overestimated due to contributions from dielectric absorption.

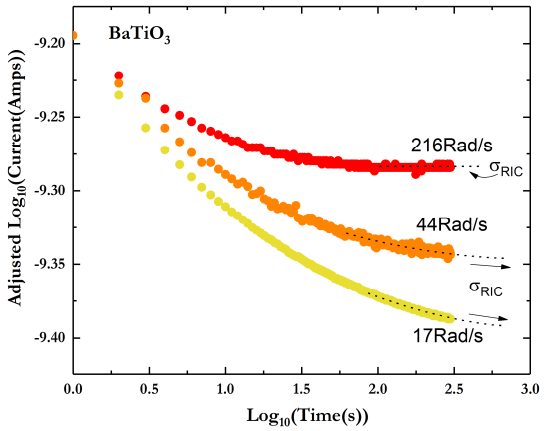

Fig. 3. Log current vs Log time for $BaTiO_3$ after voltage application under different gamma dose rates. Initial currents adjusted to be equal at t=0. Sufficient time is needed to allow dielectric absorption to settle before σ_{RIC} can be measured.

In future experiments longer hold times will be necessary to minimize the dielectric absorption contribution. Despite this, the difference between dose rates is large compared to the error from dielectric absorption, so tentative conclusions can still be drawn.

The RIC as a function of dose rate for $BaTiO_3$ and $Ba(Ce_{0.05}Ti_{0.95})O_3$ are plotted in Fig. 4. The Ce-doped $BaTiO_3$ has a reduced σ_{RIC} at all dose rates by ~30-40% compared to pure $BaTiO_3$. This is suspected to be due to the deep traps known to be formed by Ce within the band gap of $BaTiO_3$ [9].

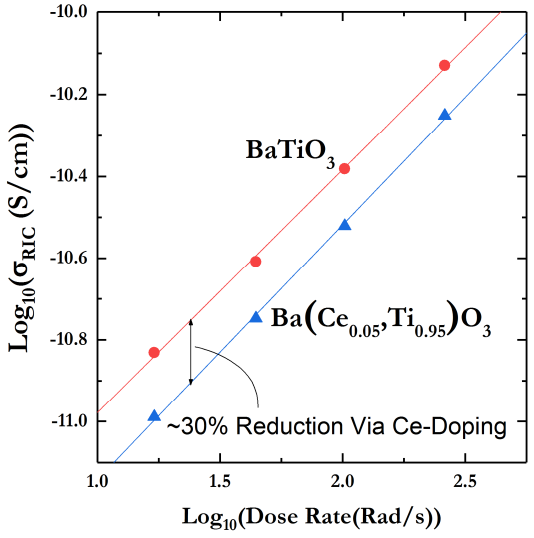

Fig. 4. Log-Log plot of Radiation Induced Conductivity vs. Dose Rate for $BaTiO_3$ and $Ba(Ce_{0.05},Ti_{0.95})O_3$. A decrease in σ_{RIC} is seen after Ce doping.

This drop is comparable to but less than the effects of dopants in other systems such as Cr and Ni in Al_2O_3 which have shown decreases in σ_{RIC} by 70-100% with much lower concentrations (~0.1mol%).[12] The current data provides experimental proof that dopants can reduce σ_{RIC} in $BaTiO_3$ based capacitors. In the current composition Ce is expected to lay on the Ti site as a neutral dopant (Ce_{Ti}^{x}) [10,13]. The neutral nature may be limiting the capture cross section of the deep trap, and a positively charged donor (correctly compensated by an acceptor) may have a larger columbic attraction to the free electrons, resulting in a much larger capture cross section and more significant decrease in σ_{RIC}.

An additional aspect of the data which should be discussed is the slope of the $Log_{10}(\sigma_{RIC})$ vs Log_{10}(Dose Rate) curve, which are 0.59 and 0.62 for $BaTiO_3$ and $Ba(Ce_{0.05},Ti_{0.95})O_3$, respectively. These are comparable slopes to photoconductivity experiments in $BaTiO_3$ [14], and the values laying between 0.5 and 1 suggest that the steady state carrier concertation is controlled by Shottky-Read-Hall recombination as opposed to direct recombination of electrons and holes [15]. This is the theoretically expected outcome for defect-heavy materials such as doped $BaTiO_3$ and $BaTiO_3$ made via conventional powder processing. However, these slopes should be interpreted with some caution. Lower dose rates were not allowed to completely settle for high accuracy σ_{RIC} determination (Fig. 3 and discussion), and other effects such as the effect of changing electric fields during IV measurements on the geminate recombination rate and the effect of voltage history on dielectric absorption contributions have not been explored fully. Future work will include work toward detangling these mixed contributions to time dependent conductivity measurements under ionizing dose.

Finally, it should be reiterated that both permittivity and σ_{RIC} are pertinent to minimizing capacitor self-discharge under accumulated dose.

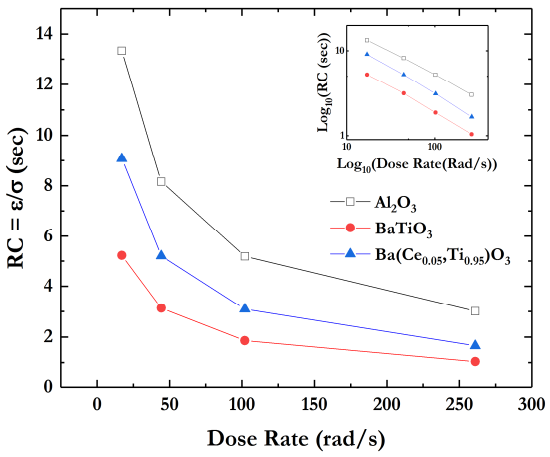

Fig. 5. RC time constant for pure $BaTiO_3$, doped $BaTiO_3$, and Al_2O_3 as a function of dose rate. The data is also plotted on log-log axes (inset) and is linear .

This is easily seen in Fig. 5 where the RC time constant as a function of dose rate is plotted for pure and doped

$BaTiO_3$ as compared to a commercial Al_2O_3 sample obtained from Coorstek. Similar RC time constants are found for all samples despite the large difference between $BaTiO_3$-based samples and Al_2O_3 in relative permittivity (~3000 vs ~10, respectively) and conductivity under gamma irradiation ($\sim 10^{10}$-10^{11} vs. $\sim 10^{-12}$-10^{-13}, respectively). The permittivity of $BaTiO_3$ is relatively unchanged with the addition of 5% Ce_{Ti}^{x}, while the leakage is significantly decreased. The RC time constant therefore increases compared to pure $BaTiO_3$. During further exploration of dopants to decrease σ_{RIC} in $BaTiO_3$, the effect of these dopants on permittivity and ferroelectric polarization should be kept in mind.

4. CONCLUSIONS

The radiation induced conductivity in $BaTiO_3$ and $Ba(Ce_{0.05},Ti_{0.95})O_3$ were measured under multiple gamma ray dose rates. The dose-rate exponent of the radiation induced conductivity suggests Shottky-Read-Hall carrier recombination, but further work is necessary to unequivocally confirm this. Ce-doping was found to effectively decrease radiation-induced conductivity, and is likely due to the present of deep traps made by Ce_{Ti}^{x} defects.

5. REFERENCES

[1] S. A. Yang, B. H. Kim, M. K. Lee, G. J. Lee, N-H. Lee, S. D. Bu, Thin Solid Films, **562**, 185-189 (2014).

[2] J. M. Benedetto, R. A. Moore, F. B. McLean, and P. S. Brody, IEEE Trans. Nucl. Sci., **37,** 1713-17 (1990)

[3] J. Gao, L. Zheng, B. Huang, Z. Song, L. Yang, Y. Fan, D. Zhu, and C. Lin, Semicond. Sci. Technol., **14**, No. 9, 836-39 (1999)

[4] S. C. Lee, G. Teowee, R. D. Schrimpf, D. P. Birnie, D. R. Uhlmann, K. F. Galloway, IEEE Trans. Nucl. Sci., **39**, No. 6, 2026-43 (1992)

[5] R. W. Klaffky, B. H. Rose, A. N. Goland, and G. J. Dienes, Phys. Rev. B., **28**, No. 8, 3610-34 (1980)

[6] M. C. Tarun, F. A. Selim, and M. D. McCluskey, Phys. Rev. Lett., **111**, 187403 (2013)

[7] R. C. Hughes, J. Chem. Phys., **55**, 5442-47 (1971)

[8] L. W. Hobbs, F. W. Clinard, S. J. Zinkle, and R. C. Ewing, J. of Nuc. Mat., **216**, 291-321 (1994).

[9] S. X. Dou, H. Song, M. Chi, Y. Zhu, and P. Ye, Proceedings Vol. 3554 Photorefractive Materials: Phenomena and Related Applications II (1998).

[10] Z. Jing, Z. Yu, C. Ang, J. Mater. Res., **38**, 1057-1061 (2003).

[11] W. Kesternich, J. Mater. Res., **15**, 11, 2280-2283 (2000).

[12] K. Shiiyama, A. Shiraishi, M. Kutsuwada, S. Matsumura, and C. Kinoshita, J. of Nuc. Mat., **329-333**, 1520-23 (2004).

[13] D. Makovec, Z. Masmardzija, and D. Kolar, J. of Solid State Chem., **123**, 30-38 (1996).

[14] D. Mahgerefteh and J. Feinberg, Phys. Rev. Lett., **64**, 2195-98 (1990)

[15] K. C. Kao, Dielectric Phenomena in Solids, Elsevier Academic Press, London, UK, 480-514